

# Constructing band diagrams of semiconductor heterojunctions

Cite as: Appl. Phys. Lett. **66**, 457 (1995); <https://doi.org/10.1063/1.114055>

Submitted: 02 June 1994 • Accepted: 10 November 1994 • Published Online: 04 June 1998

M. Leibovitch, L. Kronik, E. Fefer, et al.



View Online



Export Citation

## ARTICLES YOU MAY BE INTERESTED IN

[Determining band offsets using surface photovoltage spectroscopy: The InP/In<sub>0.53</sub>Ga<sub>0.47</sub>As heterojunction](#)

Applied Physics Letters **69**, 2587 (1996); <https://doi.org/10.1063/1.117708>

[Detailed Balance Limit of Efficiency of p-n Junction Solar Cells](#)

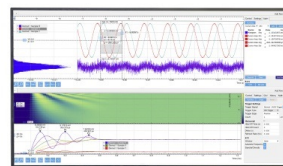
Journal of Applied Physics **32**, 510 (1961); <https://doi.org/10.1063/1.1736034>

[Surface photovoltage spectroscopy of thin films](#)

Journal of Applied Physics **79**, 8549 (1996); <https://doi.org/10.1063/1.362535>

## Challenge us.

What are your needs for periodic signal detection?



Zurich  
Instruments

# Constructing band diagrams of semiconductor heterojunctions

M. Leibovitch, L. Kronik, E. Fefer, V. Korobov, and Yoram Shapira<sup>a)</sup>

Department of Electrical Engineering-Physical Electronics, Faculty of Engineering, Tel-Aviv University, Ramat-Aviv 69978, Israel

(Received 2 June 1994; accepted for publication 10 November 1994)

A novel approach for constructing the band diagrams of semiconductor heterojunctions is discussed and illustrated. It is based on a simple measurement of band discontinuities, Debye length and the width of the space-charge region at the heterojunction interface. Monitoring the changes in the surface potential during heterojunction formation makes it possible to identify the contributions of the interface states and dipole. The approach is illustrated by the results of experiments performed on the InP/In<sub>2</sub>O<sub>3</sub> heterojunction. © 1995 American Institute of Physics.

The extraordinary success of low-dimensionality semiconductor heterostructures has attracted vast efforts in both fundamental and applied physics.<sup>1</sup> The electrical characteristics of such structures and devices are critically dependent on the heterojunction band structure, which plays an important role in transport phenomena. The transition between the two materials at the heterojunction interface causes energy discontinuities in the conduction and valence bands,  $\Delta E_c$  and  $\Delta E_v$ , in the vicinity of the metallurgical junction.<sup>2,3</sup> In addition, a dipole layer may appear at the junction,<sup>4</sup> and various kinds of imperfections at the interface may result in interface charge.<sup>5</sup> Due to the band discontinuities, the interface charge, dipole, and a possible change in the net doping concentrations at the junction, an electric field appears at the junction. We define the task of constructing a band diagram as finding the distribution of this field, as well as the band discontinuities. Various approaches have been developed,<sup>2-3</sup> but there is still no generally accepted method for the precise and direct measurement of the band diagram.

It is well known that for a uniform material with constant band gap and electron affinity the band discontinuities may be expressed in the following form:<sup>2</sup>

$$\begin{aligned}\Delta E_c &= E_{c1} - E_{c2} - eV_{bi}, \\ \Delta E_v &= E_{v1} - E_{v2} - \Delta E_c,\end{aligned}\quad (1)$$

where  $E_{c1}$ ,  $E_{c2}$  are relative positions of the edges of conduction bands of the two materials with respect to the Fermi level in the quasineutral region far away from the heterojunction,  $E_{v1}$ ,  $E_{v2}$  are the band gaps, and  $V_{bi}$  is the built-in voltage of the junction. Equation (1) uses the following sign conventions:  $V_{bi}$  follows the usual sign convention of an electrostatic potential, which is positive if the potential in the quasineutral region of material 2 is higher than in that of material 1, i.e., it is positive if the bands are bent down from material 1 to material 2.  $\Delta E_c$  is positive if the bottom of the conduction band drops on passing from material 1 to material 2, whereas  $\Delta E_v$  is negative if the top of the valence band drops on passing from material 1 to material 2. Since  $E_c$  and  $E_v$  are bulk parameters of the two materials, and may be measured by a host of well-known techniques,<sup>6</sup> the problem of determining the band discontinuities is equivalent to the

problem of measuring the built-in voltage at the junction. The total voltage drop (built-in voltage) at the interface is clearly given by:

$$V_{bi} = V_{b1} + V_{b2} + \Delta\phi_{in}, \quad (2)$$

where  $V_{b1}$  and  $V_{b2}$  are the band-bending voltages on each side of the interface, and  $\Delta\phi_{in}$  is the potential step due to dipoles at the metallurgical junction,<sup>4</sup> all of which also obey the electrostatic potential sign convention.

The ratio between  $V_{b1}$  and  $V_{b2}$  is determined by charge balance considerations, which may be expressed by the equation:

$$Q_1 + Q_2 + Q_{in} = 0, \quad (3)$$

where  $Q_1$  and  $Q_2$  are the charge densities (per unit area) on each side of the interface, and  $Q_{in}$  is the interface charge density. The effect of the dipole on this balance is negligible because the thickness of the dipole layer is much smaller than the total width of the space-charge region and hence the dipole may be considered as a quasineutral electrostatic system. The relation between the band-bending voltage and the corresponding electric charge may be obtained by solving the Poisson equation.

In the following, we show that if the surface potential ( $V_s$ ) is monitored during the formation of the heterojunction,  $V_{bi}$  and the charge densities may be found. Hence, the band diagram may be constructed.

We assume that the substrate surface properties (local states and dipole)<sup>7</sup> are modified to the interface properties upon the initial stages of the growth, and remain fixed henceforth, i.e., the charge of these states does not change with the layer thickness either. Both sides of the interface are assumed to be depleted. We wish to emphasize that this approach may be applied equally well to other cases, the case in question being merely an illustrative, yet important example, which lends itself to analytical formulation.

We first consider an ideal case, in which the initial substrate surface is free of surface states and dipole and the external surface has no dipole. In the case under consideration the overlayer is fully depleted, and there is no electric field in the neutral part of the substrate, i.e.,  $dV(w)/dx = 0$ , where  $w$  is the width of the total depletion region (the position of the surface is  $x = 0$ ). We also choose  $V(w) = 0$ . Since

<sup>a)</sup>Electronic mail: shapira@eng.tau.ac.il

the dielectric constant is different in the substrate and in the overlayer, let us solve the general form of the one-dimensional Poisson equation, namely:

$$\frac{d}{dx} \left( \epsilon(x) \frac{dV(x)}{dx} \right) = -\rho(x), \quad (4)$$

where  $\rho(x)$  is the charge density in the depletion region and  $\epsilon(x)$  is the permittivity. For uniform charge densities under the depletion approximation, the charge density is  $\rho_l$  in the overlayer, and  $\rho_s$  in the space charge region of the substrate. At the substrate/layer interface, the surface-charge density  $Q_{in}$  and the interface dipole  $\Delta\phi_{in}$ , dictate the following boundary conditions:

$$V(w_0^-) = V(w_0^+) + \Delta\phi_{in}, \quad (5a)$$

$$\epsilon_l \frac{dV(w_0^-)}{dx} = \epsilon_s \frac{dV(w_0^+)}{dx} + Q_{in}, \quad (5b)$$

where  $w_0$  is the thickness of the overlayer,  $w_0^-(w_0^+)$  is the coordinate just above (below) the interface, and  $\epsilon_s(\epsilon_l)$  is the dielectric constant of the substrate (layer). Before a quasineutral region is formed in the growing layer, charge conservation requires that the surface charge density be equal and opposite to the total charge per unit area in the depletion region, and thus:

$$Q_{ex} = -Q_{sc} = -\int_0^w \rho(x) dx, \quad (6)$$

where  $Q_{ex}$  denotes the charge density on the free surface of the layer, and  $Q_{sc}$  is the total charge (per unit area) in the depletion region. After integrating Eq. (4) twice and using Eqs. (5) and (6), we obtain:

$$V_s \equiv V(0)$$

$$= -\frac{\rho_l}{2\epsilon_l} w_0^2 - \frac{Q_{in}}{\epsilon_l} w_0 + \Delta\phi_{in} - \frac{Q_{ex} + \rho_l w_0 + Q_{in}}{2\epsilon_s} \\ \times \left( \frac{Q_{ex} + \rho_l w_0 + Q_{in}}{\rho_s} - 2w_0 - \frac{2(\epsilon_s - \epsilon_l)w_0}{\epsilon_l} \right). \quad (7)$$

Equation (7) clearly shows that the variation of the layer thickness and/or of any of the charge densities induces changes in the surface potential. In the extreme case where  $Q_{in}$ ,  $Q_{ex} \ll \rho_l w_0$ , the surface potential changes with the layer thickness as  $V_s \propto w_0^2$ , and in the opposite extreme case this dependence is linear, i.e.,  $V_s \propto w_0$ .

When the layer thickness becomes comparable with the width of the depletion region in the layer ( $w_l$ ), the depletion approximation can no longer be utilized, and the screening effect of the free carriers must be taken into account. For such thicknesses, the expression for  $\rho(x)$  must be modified to:<sup>8</sup>

$$\rho(x) = \rho_l (1 - e^{\pm eV(x)/kT}), \quad (8)$$

where Boltzmann statistics is used for the free carriers. If  $w_0 \approx w_l$ , such that the inequality  $|V(w_0) - V(w_l)| < kT/e$  holds, the solution of the Poisson equation is well known to be

$$|V(w_0) - V(w_l)| \propto e^{-|w_0 - w_l|/l_D}, \quad (9)$$

where  $l_D$  is the Debye length of the layer, and is given by:

$$l_D = \sqrt{\frac{kT\epsilon_l}{e^2 N_l}}, \quad (10)$$

where  $N_l$  is the net (volume) free carrier charge density in the layer.

If the layer thickness becomes greater than the depletion region width in the layer, the total change of the surface potential attains its saturation value  $\Delta V_{sat}$ , which, in this ideal case, is exactly equal to the sum of the built-in voltage across the heterojunction and the band bending at the external surface, which may be determined separately.

In the general case, where the free surface of the initial substrate and the external surface of the overlayer may have local states and dipoles, the built-in voltage of the junction may be expressed as the following sum:

$$V_{bi} = (V_b^{sub} + \Delta\phi_{sub}) + \Delta V_{sat} - (V_b^{ex} + \Delta\phi_{ex}), \quad (11)$$

where  $V_b^{sub}$ ,  $V_b^{ex}$ , and  $\Delta\phi_{sub}$ ,  $\Delta\phi_{ex}$  are the band-bending voltage and the potential step due to the dipole at the free surface of the substrate prior to the deposition, and at the external surface (of the overlayer, which is thick enough to avoid coupling of the heterojunction and external interface), respectively. Both values may be obtained from independent experiments. The band-bending voltage may be found, for example, by means of the photosaturation technique.<sup>9</sup> Since the dipole is generally a direct result of the ordering of the surface,<sup>7</sup> it may be measured by subtracting the surface band bending from the difference in the work function before and after order-disorder (or vice versa) transition of the surface. Use of such procedures has been reviewed and discussed by Monch.<sup>7</sup> Once all values on the right side of Eq. (11) are measured independently, the built-in voltage is easily found.

The interpretation of the dependence of the surface voltage on the layer thickness, which relies upon Eqs. (7)–(11), yields the built-in voltage, the width of the depletion region and the Debye length in the layer, as well as charge densities. In the case under consideration, the charge density in the layer  $Q_2$  is given simply by the product  $\rho_l w_l$ , and thus it is also found from the measurement. Moreover,  $Q_{in}$  may be found by fitting the  $V_s(w_0)$  curve with Eq. (7). The magnitude of  $Q_{ex}$  may be separately determined if the overlayer is grown up to such a thickness that all interface features are screened. Once  $Q_{in}$  and  $Q_2$  are known, finding  $Q_1$  from Eq. (3) is a trivial matter. When all charges are known, the band bendings on each side of the interface may be found by the following Poisson relation:<sup>8</sup>

$$V_{b1,2} = \frac{Q_{1,2}^2}{2\epsilon_{1,2}\rho_{1,2}}, \quad (12)$$

and finally, the dipole contribution to the band bending may be found by means of Eq. (2), which also serves as a simple technique for the verification of the existence of an interface dipole.

Obviously, a more comprehensive analysis is possible within the framework of a numerical model,<sup>10,11</sup> which is free of the simplifying assumptions utilized above. The results of the numerical simulation fully support the predic-

tions of Eqs. (7)–(12). Reconstruction of the band diagram shows a good agreement with the assumed values. Moreover, examination shows that the present approach may be used for any type of semiconducting materials.

As an experimental example, we demonstrate our approach by constructing the band diagram of the  $\text{In}_2\text{O}_3/p\text{-InP}$  interface. This  $p\text{-}n^+$  heterojunction (type II) has been chosen since its properties are very close to a Schottky diode, and thus any band bending is essentially restricted to the semiconducting InP. Therefore, the results obtained may be correlated with the Schottky barrier height, as measured by the standard  $I$ – $V$  technique. Furthermore, the etching processes of the free surface prior to growth and the polycrystalline nature of the growth induce a disorder which is significant enough to make it possible to neglect the effect of surface dipoles.<sup>7</sup>

The samples used in the experiment were (100) oriented  $p$ -type InP wafers (Zn doped,  $5 \times 10^{16} \text{ cm}^{-3}$ ). The initial band bending was found to be 225 mV by means of the photosaturation technique.<sup>9</sup> Consequently, the contact potential difference (CPD) was measured *ex situ* at various stages of  $\text{In}_2\text{O}_3$  growth. Details of the growth process<sup>12</sup> and the CPD measurement<sup>13,14</sup> may be found elsewhere. The resultant change in the CPD was found to be 535 mV. Therefore, the built-in voltage is 760 mV. For the InP substrate,  $E_{c1}$  is 1.21 eV, and for the  $\text{In}_2\text{O}_3$ ,  $E_{c2}$  was found to be 0.013 eV. Due to the high doping, the band bending at the external surface is negligible. This gives a value of 0.44 eV for  $\Delta E_c$ . Using 1.34 and 3.5 eV as the band gaps of InP and  $\text{In}_2\text{O}_3$ , respectively, a corresponding value of  $-2.60 \text{ eV}$  for  $\Delta E_v$  is found. Because the growth process of the  $\text{In}_2\text{O}_3$  is significantly two dimensional,<sup>12</sup> the experimental curve cannot be fitted by the simplistic relation in Eq. (7). Nevertheless, some quantitative considerations are still fruitful: The measured

dependence  $V_s(w_0)$  shows that  $V_s$  attains its saturation value at an overlayer thickness of about 100 Å, i.e., the depletion region in the layer is very small, and hence the depletion approximation is valid only for the very initial stages of growth. The doping concentration in the layer is about  $1.3 \times 10^{18} \text{ cm}^{-3}$ . This estimate is obtained from a Debye length of  $l_D \approx 33 \text{ Å}$ , which is measured by fitting the measured  $V_s(w_0)$  dependence with Eq. (9). The Schottky barrier, as calculated from these data, is 0.89 eV. This value is within 6% of the independently ( $I$ – $V$ ) measured value of 0.84 eV, and the accuracy can doubtlessly be improved even further if *in situ* measurements are performed. Using the bulk parameters and doping of the two materials, and the measured band discontinuity, the Poisson equation has been solved numerically. Indeed, a value of 100 Å has been obtained for the depletion region width in the  $\text{In}_2\text{O}_3$ . Moreover, it yields the value of 1460 Å for the depletion region width in the InP, and balance of charge considerations show that the interface dipole is indeed negligible. Thus, the entire InP/ $\text{In}_2\text{O}_3$  band diagram has been constructed, and is shown in Fig. 1.

In conclusion, we have presented a simple technique for constructing the band diagrams at semiconductor interfaces, which also makes it possible to identify the contributions of different physical mechanisms. The approach, which is based on monitoring changes in the surface potential is usually simple to apply, contactless, nondestructive, suitable for *in situ* measurements as well, and may be used for any type of semiconducting materials.

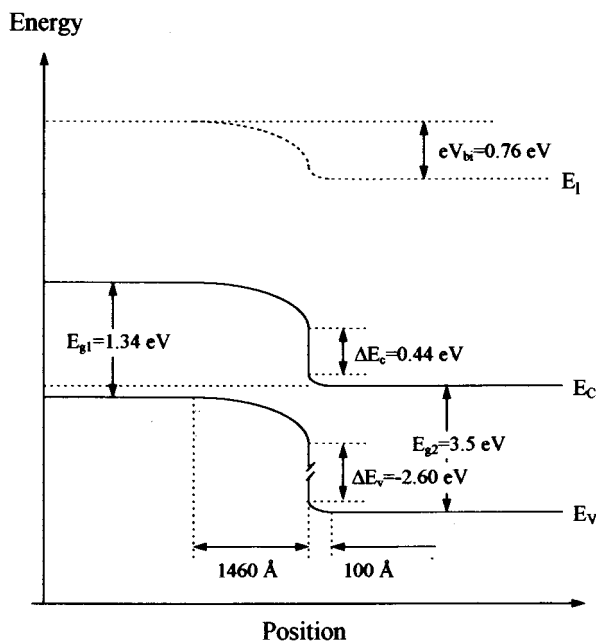


FIG. 1. Band diagram of the  $\text{In}_2\text{O}_3/p\text{-InP}$  interface.

<sup>1</sup>C. Weisbuch and B. Vinter, *Quantum Semiconductor Structures* (Academic, San Diego, CA, 1991).

<sup>2</sup>*Heterojunction Band Discontinuities*, edited by F. Capasso and G. Margaritondo (North-Holland, Amsterdam, 1987), and references therein.

<sup>3</sup>For an overview on the current state of the art in this field, see the Proceedings of the 20th Annual Conference on the Physics and Chemistry of Semiconductor Interfaces, Williamsburg (1993), and references therein [J. Vac. Sci. Technol. B **11**, (1993)].

<sup>4</sup>J. Tersoff, Phys. Rev. Lett. **56**, 2755 (1986); J. Tersoff, Phys. Rev. B **30**, 4874 (1984).

<sup>5</sup>G. Lelay, J. Derrien, and N. Boccaro, *Semiconductor Interfaces: Formation and Properties*, Springer Proceedings in Physics Vol. 22 (Springer, Berlin, 1987).

<sup>6</sup>D. K. Schroder, *Semiconductor Materials and Device Characterization* (Wiley, New York, 1990).

<sup>7</sup>W. Monch, in *Chemistry and Physics of Solid Surface V*, Springer Series in Chemical Physics, Vol. 35, edited by R. Vanselow and R. Howe (Springer, Berlin, 1984).

<sup>8</sup>S. M. Sze, *Physics of Semiconductor Devices* (Wiley, New York, 1985).

<sup>9</sup>L. J. Brillson and D. W. Kruger, Surf. Sci. **102**, 518 (1981).

<sup>10</sup>G. Ashkinazi, M. Leibovitch, and M. Nathan, IEEE Trans. Electron Devices **ED-40**, 285 (1993).

<sup>11</sup>M. Leibovitch, L. Kronik, E. Fefer, and Y. Shapira, Phys. Rev. B **50**, 1739 (1994).

<sup>12</sup>V. Korobov, Y. Shapira, B. Ber, K. Faleev and D. Zushinskiy, J. Appl. Phys. **75**, 2264 (1994).

<sup>13</sup>W. Thomson, Philos. Mag. **5**, 46 (1898).

<sup>14</sup>D. P. Woodruff and T. A. Delchar, *Modern Techniques of Surface Science* (Cambridge University Press, Cambridge, 1986), Chap. 7, pp. 368–372.